Proceedings of the ASME 2018
Conference on Smart Materials, Adaptive Structures and Intelligent Systems
SMASIS2018
September 10-12, 2018, San Antonio, TX, USA

SMASIS2018-8097

DESIGN, DEVELOPMENT AND CHARACTERIZATION OF LINEAR, SOFT ACTUATORS VIA ADDITIVE MANUFACTURING

Alfonso Costas
School of Mechanical Engineering,
Purdue University
West Lafayette, Indiana, USA

Daniel E. Davis
School of Engineering Technology,
Purdue University
West Lafayette, Indiana, USA

Yixian Niu
Department of Agricultural and Biological Engineering,
Purdue University
West Lafayette, Indiana, USA

Sadegh Dabiri
Department of Agricultural and Biological Engineering,
School of Mechanical Engineering
Purdue University
West Lafayette, Indiana, USA

Jose Garcia
School of Engineering Technology,
Purdue University
West Lafayette, Indiana, USA

Brittany Newell
School of Engineering Technology,
Purdue University
West Lafayette, Indiana, USA

ABSTRACT

Additive manufacturing has emerged as an alternative to traditional manufacturing technologies. In particular, industries like fluid power, aviation and robotics have the potential to benefit greatly from this technology, due to the design flexibility, weight reduction and compact size that can be achieved. In this work, the design process and advantages of using 3D printing to make soft linear actuators were studied and highlighted. This work explored the limitations of current additive manufacturing tolerances to fabricate a typical piston-cylinder assembly, and how enclosed bellow actuators could be used to overcome high leakage and friction issues experienced with a piston-cylinder type actuator. To do that, different 3D printing technologies were studied and evaluated (stereolithorgraphy and fused deposition modeling) in the pursuit of high-fidelity, cost-effective 3D printing. The initial attempt consisted of printing the soft actuators directly using flexible materials in a stereolithography-type 3D printer. However, these actuators showed low durability and poor performance. The lack of a reliable resin resulted in the replacement of this material by EcoFlex® 00-30 silicone and the use of a 3D printed mold to cast the actuators. These molds included a 3-D printed dissolvable core inside the cast actuator in order to finish the manufacturing process in one single step. An experimental setup to evaluate the capabilities of these actuators was developed. Results are shown to assess the steady-state and the dynamic characteristics of these actuators. These tests resulted into the stroke-pressure and stroke-time responses for a specific load given different proportional valve inputs.

INTRODUCTION

Piston-cylinder assemblies are typically seen in industry when using traditional manufacturing methods [1]. However, the tight tolerances associated to the function of these parts are a serious challenge to replicate in 3D printed components. The circular shape of the actuator makes this even more challenging, since the digital nature of the 3D printing files creates a discretized polygon shape rather than an actual, smooth circle [2]. This makes it difficult to achieve a proper compromise between friction and sealing when performing linear actuation. In the interest of reducing friction and leakage, it is possible to create a bellows-like soft actuator where all fluid can be enclosed within a specific volume. In addition, there are many advantages to using soft actuators such as their ease of fabrication and operation, low cost, and their high power-to-weight ratio. This

Copyright © 2018 ASME

Downloaded From: https://proceedings.asmedigitalcollection.asme.org on 11/20/2018 Terms of Use: http://www.asme.org/about-asme/terms-of-use

work evaluated different ways in which it is possible to use additive manufacturing technology in order to create bellows actuators. This involved two methods: The first one consisted of 3D printing the bellows actuator directly using stereolithography printing, and the second method consisted of 3D printing a mold via Fused Deposition Modeling (FDM), and using a silicone-rubber mix (in this case, EcoFlex® 00-30) to cast these actuators. The objectives of this work were to showcase the process involved in fabricating these actuators using the aforementioned methods and to quantify the steady-state and dynamic response of the actuators experimentally.

BACKGROUND

Many researchers have 3D printed soft actuators using stereolithography. Slightam and Gervasi [2] mentioned the difficulties related to 3D printing a piston-cylinder assembly and suggested the use of diaphragms or bellows-type actuators. They defined solid state actuators (SSA) as single, multi-functional components made of diaphragms, bellows, springs, etc. MacCurdy et al. [3] used solid and liquid materials to print a robot with six bellows-actuated legs. Peele et al. [4] developed a soft pneumatic actuator using a bellows structure via a digital projection stereolithography (DMP-SL) process. They split the internal chamber of their actuator into four in order to have a higher degree of flexibility over their actuation direction. In addition to the use of 3D printing to create soft structures, researchers have used other types of soft materials to make soft actuators. Belforte et al. [5] showcased some of the applications of soft robotics for rehabilitation equipment. In their work, actuators were tested to compare performance during contraction or expansion while varying muscle supply pressure and applied load. Agarwal et al. [6] developed fiber-reinforced actuators which, after testing over 1200 cycles, showed no Mullins effect, demonstrating that these actuators offer great repeatability improvement over previously designed prototypes. These results were based on experiments and numerical methods with close agreement amongst them.

METHODS

1. Fabrication of a soft actuator using stereolithography printing

The first methodology consisted of using stereolithography technology to 3D print soft actuators directly. These actuators were developed using two types of 3D printers: The Formlabs Form 2 and the Autodek Ember. The Form 2 3D printer provides a build size of 15×15×18 cm^3 with a laser point size of 140 microns while the Ember printer has a build size of 6×4×16 cm^3 with a maximum resolution of 50 microns. These printers allowed for the use of flexible resins as well as hard resins. First, a model was printed using Formlabs' Flexible resin only, as shown in Figure 1.

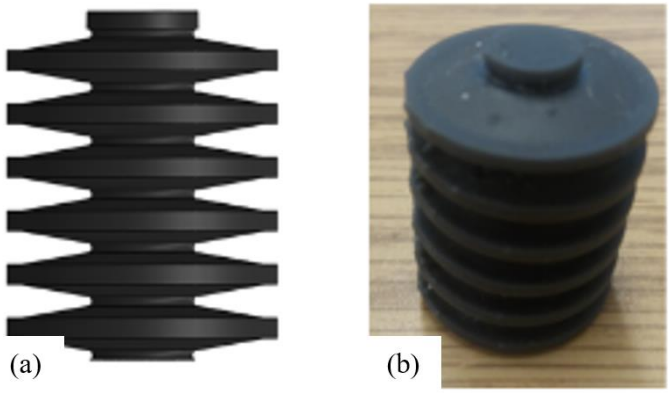

Figure 1. 3D printing of a soft actuator using flexible resin in the Form 2 3D printer. Figure 1 (a) represents the CAD prototype and Fig.1 (b) shows the 3D printed version.

However, these actuators were not durable enough for the application and broke quickly when performing a few actuations. Therefore, the use of this material needed to be revisited. The Form 2 printer was capable of printing mixtures of resins from the Formlabs resin catalogs while still obtaining successful prints. A few iterations were carried out in order to obtain the right resin mix and print parameters. Two types of 3D printing resins were used: Formlabs Clear and Formlabs Flexible. The material properties of these two resins (as provided by the resin manufacturer) are outlined in Table 1.

Table 1. Resin properties for Formlabs Clear and Formlabs Flexible.

Parameter	Values	
Resin Type	**Clear**	**Flexible**
Tensile Strength	65 MPa	7.7-8.5 MPa
Elongation at Failure	6.2%	75 – 85%
Young's Modulus	2.8 GPa	Not provided

In order to 3D print a bellows actuator that could meet the required functionality, it was necessary to make a component that could stretch sufficiently to meet the required stroke without breaking. This required stroke was defined to be 50% of the actuator's initial 100 mm length. In addition, these actuators needed to be able to sustain cyclic loading without breaking. Therefore, it was necessary to determine which material provided the best compromise between stroke and durability. Overall, four mixtures were created with different compositions ranging from 50% flexible resin and 50% clear resin to 75% flexible resin and 25% clear resin. These limits were established based on the fact that any mix with a Formlabs Clear resin concentration higher than 50% resulted in insufficient stroke while a concentration lower than 25% resulted in the actuator breaking too quickly. For each composition, an actuator was printed and its stroke and durability were evaluated. Using a higher percentage of flexible material resulted in a longer stroke while using a higher percentage of hard resin material resulted in

Copyright © 2018 ASME

Downloaded From: https://proceedings.asmedigitalcollection.asme.org on 11/20/2018 Terms of Use: http://www.asme.org/about-asme/terms-of-use

better durability. Figure 2 and Figure 3 show two different compression lengths associated with different material mixtures. Figure 2 shows a bellows actuator with 50% flexible resin and 50% clear resin, and Figure 3 shows an actuator with 75% flexible resin and 25% clear resin.

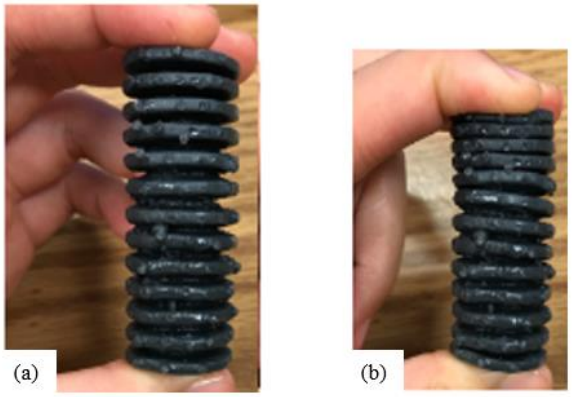

Figure 2. Bellows actuator with 50% flexible resin and 50% clear resin. Figure.2 (a) shows the actuator before compression and Fig.2 (b) shows the actuator after compression.

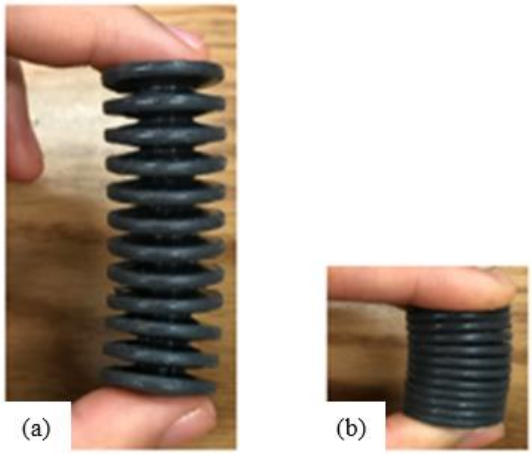

Figure 3. Bellows actuator with 75% flexible resin and 25% clear resin. Figure 3 (a) shows the actuator before compression and Fig.3 (b) shows the actuator after compression.

Unfortunately, the prototypes that provided the adequate level of actuation broke after a few cycles. The prototypes that did not break were too stiff to provide the required stroke. Several attempts were performed in order to alter the actuator geometry and print settings. However, these attempts proved to be unsuccessful as well. Therefore, it was concluded that the above materials and methodologies did not provide the required durability and stroke requirements for the flexible bellows actuators.

2. Fabrication of a soft actuator using an FDM mold and Ecoflex 00-30 silicone

The next approach involved printing a mold via FDM and using Ecoflex® 00-30 to cast an actuator. Several commercial silicone rubbers are available in the market at an affordable price. The materials were selected based on the recommendations of Agarwal et al [6]. They studied the use of Ecoflex® 00-10, Ecoflex® 00-20, Ecoflex® 00-30, Elastosil® and Dragonskin®. According to their work, Ecoflex® 00-10 and Ecoflex® 00-20 were not robust enough (unable to maintain pressures of up to 50 kPa without breaking or leaking) when compared to Ecoflex® 00-30. Also, the use of Elastosil®, and Dragonskin® required higher pressures to begin actuation (greater than 85 kPa), which were too high for the scope of this project. Therefore, Ecoflex® 00-30 was used for this work. This material has a tensile strength of 200 psi and an elongation at break of 900%. In addition, this material was fully characterized by Case et al., [7] and their results provide a reference for the experimental work.

First Mold Iteration:

A bellows-shaped mold with a square cross section was printed using FDM technology and ABS material. The reason behind the square cross-section was to avoid excessive radial expansion. The first mold included three pieces, and the actuator was cast in a 2-step process. In order to enhance the mold release process, the surface of the FDM prints was smoothened by acetone and sprayed with Ease Release®.

Figure 4. 2-step mold FDM parts.

The first step consisted of coupling the core (piece to the left in Figure 4) and the outside body (piece to the right in Figure 4) of the mold and casting the silicone mix. This mix was cured in 4 hours at ambient temperature. The second step consisted of casting the missing actuator front cover to the rest of the geometry by placing the cured actuator section on top of the resin deposited in the front cover (center piece in Figure 4). This process is outlined in Figure 5.

Copyright © 2018 ASME

Downloaded From: https://proceedings.asmedigitalcollection.asme.org on 11/20/2018 Terms of Use: http://www.asme.org/about-asme/terms-of-use

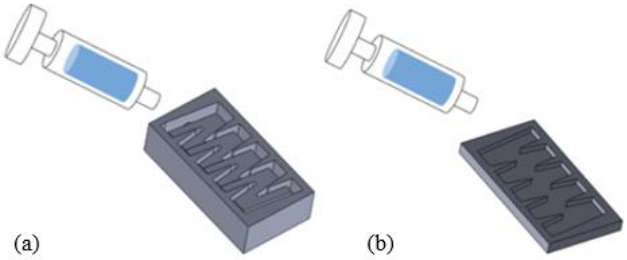

Figure 5. FDM mold casting process. Figure 5 (a) shows the first step of the 2-step mold process and Fig.5 (b) shows the second step.

During the testing phase of these actuators, it was observed that the actuator side that was made during the second step in the casting process started to detach due to a poor alignment of the silicone during casting in the second step. This alignment was difficult to control and was not free of errors.

Second Mold Iteration:

To resolve the issue presented in the two step casting process, an alternative approach was designed to make the silicone pouring process one step. This was done by fabricating a soluble actuator core (using commercially available soluble filaments), placing it inside the outer mold, and then pouring all the silicone in one step. After this, the core inside the actuator was dissolved. Two different dissolvable core materials were tested. The first one was a d-limonene soluble high impact polysterene (HIPS) filament. However, the reaction between the d-limonene solvent and the silicone damaged the actuator, resulting in the cured silicone degradation shown in Figure 6.

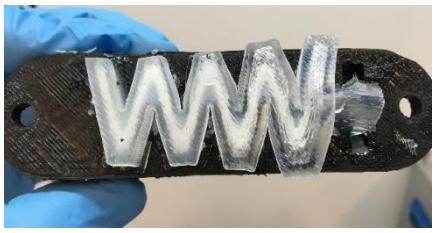

Figure 6. Result of silicone actuator after submerging it in d-limonene solvent for one hour.

The second test material used to produce the core was a water-soluble PVA filament. This material worked well, as it was possible to dissolve the core within the actuator by placing it in a warm bath of water for 45 minutes. This step concluded the soft actuator development process. An outline of the sequence involved in fabricating these actuators is shown in Fig. 7.

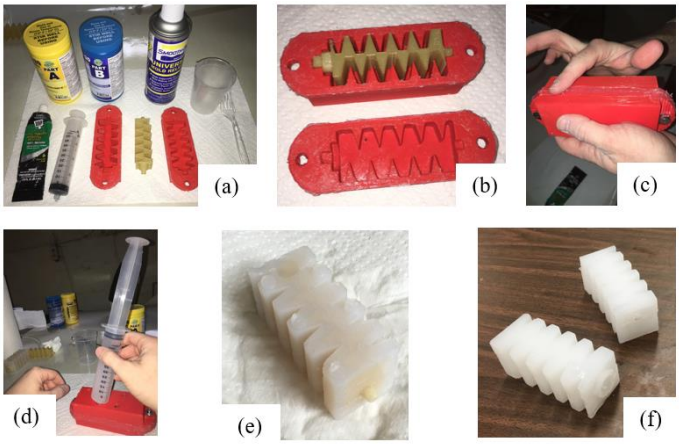

Figure 7. Actuator fabrication process. Figure 8 a) displays the preparation of materials before making the mold. Figure 8 b) shows the 3 individual mold pieces and Fig. 8 c) shows the assembly of the mold pieces and sealing process. Figure 8 d) shows the pouring process of Ecoflex ® 00-30 in the mold. Figure 8 e) shows the actuator with the core inside before it has been dissolved and Fig. 8 e) displays the final actuator results after the core has been dissolved.

The pictures shown in Figure 7 demonstate the extended and relaxed shapes of the flexible actuator produced by the second casting fabrication method.

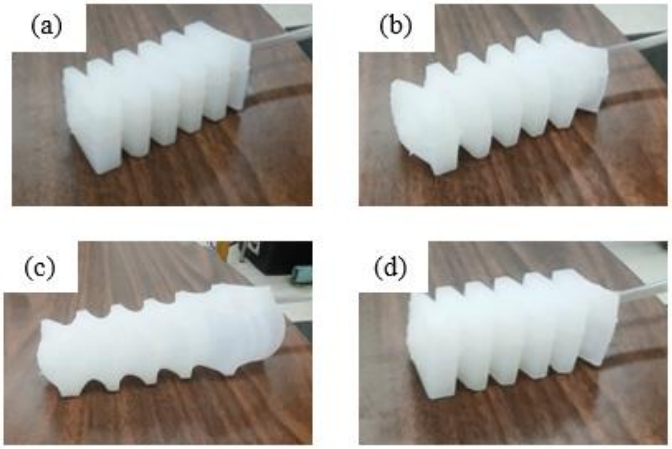

Figure 7. Example of actuation. Figure 9 a) shows the initial position. Figure 9 b) shows an initial actuation level while Fig. 9 c) shows the maximum actuation. Figure 9 d) shows the actuator back in its relaxed position.

Actuator Geometry:

Figure 8 shows a cutaway section of the actuator geometry, outlining its characteristic features. Notice that the hatched cross section represents the actuator's walls. After a few iterations, it was determined that a minimum wall thickness of 2.5 mm should be employed to obtain a durable actuator that would not present any orifices after the fabrication or curing process.

Copyright © 2018 ASME

Downloaded From: https://proceedings.asmedigitalcollection.asme.org on 11/20/2018 Terms of Use: http://www.asme.org/about-asme/terms-of-use

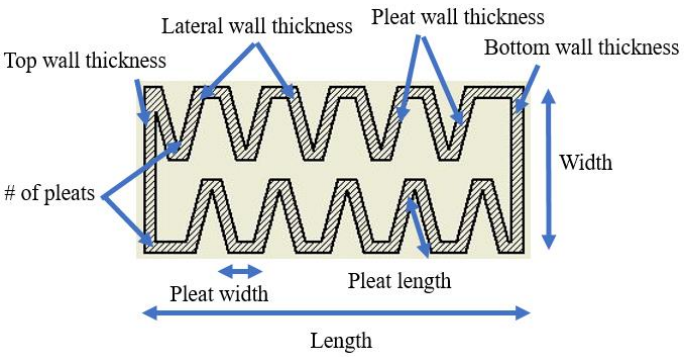

Figure 8. Cutaway section of actuator geometry

The geometric parameters of the actuator used to carry out tests is outlined in Table 2.

Table 2. Test actuator dimensions.

Parameter	*Value*
Actuator length	85.0 mm
Actuator width and thickness	37.5 mm
Pleat width	7.67 mm
Pleat length	13.88 mm
Pleat wall thickness	4.0 mm
Lateral wall thickness	4.0 mm
Top and bottom wall thickness	2.65 mm
Internal Volume	14110 mm^3
Number of pleats	4

TESTING

The next step was to create a test setup to characterize the actuator performance. The testing procedures and results are split into two sections. The first section analyzes the steady-state response of the actuator for different pressure levels and loads, resulting in a length-pressure curve for three different loading conditions. The second section evaluates the step response to a given pressure and load input, resulting in plots showing the displacement response vs. time.

Steady State Test

Three different tests were performed with three different loads: 10, 200, and 500 grams. The actuator was oriented to push the load vertically as shown in Fig. 11. For these tests, the pressure was varied in discrete steps until a steady state condition was reached. Each pressure condition was maintained constant for 60 seconds to let the pressure values stabilize. These pressures were varied both increasingly and decreasingly. Supply pressure was regulated via an electronically controlled proportional valve (ProportionAir FQPV2) so that the user could control the inlet pressure via a voltage command. The supply pressure readings were measured using a 0-15 psi pressure transmitter (WIKA 50426397) and the position data was obtained by analyzing a video taken with a digital camera (Casio EX-ZR1000) at 30 fps using Tracker, an open source computer vision software made for measuring the kinematic motion of a particle. The pressure data and the valve opening were interfaced using MATLAB® and a National Instruments USB 6221 data acquisition card, with a sampling rate of 30 samples per second. A structure to contain test weights, along with the casing to enclose the actuator, were 3D printed. Note that the casing structure helped obtain a linear actuation by limiting lateral expansion. However, this casing was also responsible for some of the friction observed in the system. Figure 9 shows a schematic of the test setup for these experiments and Fig. 10 shows the actual experimental setup.

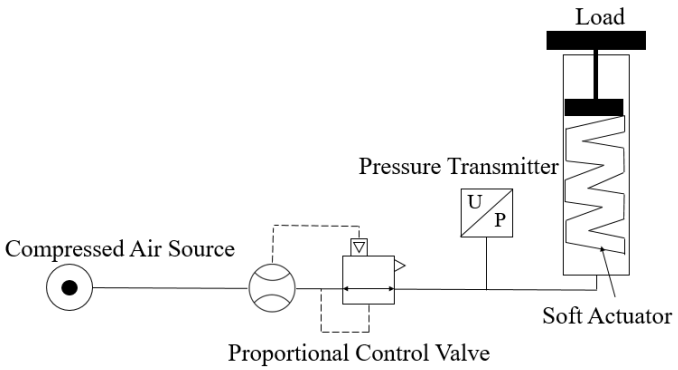

Figure 9. Schematic of the soft actuator experimental setup.

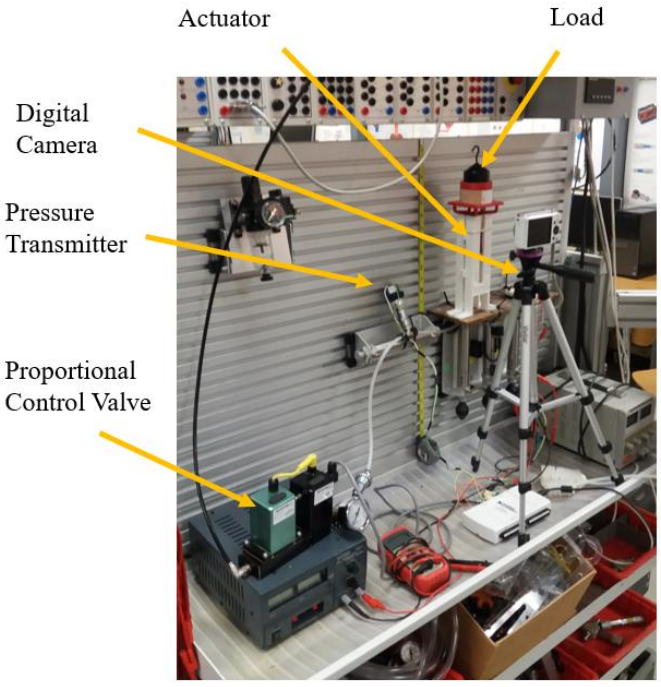

Figure 10. Soft actuator experimental setup

Copyright © 2018 ASME

Downloaded From: https://proceedings.asmedigitalcollection.asme.org on 11/20/2018 Terms of Use: http://www.asme.org/about-asme/terms-of-use

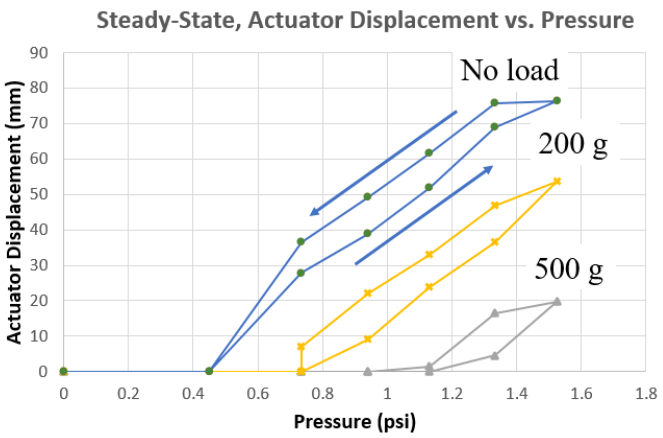

Figure 11. Position vs. pressure plot for three different loads.

Figure 11 shown above depicts the position vs. pressure results for the three different loading conditions. As the pressure was increased, the pneumatic actuator was expanded; while when pressure was reduced the actuator contracted. The arrows in Figure 11 denote the direction of actuation. As expected, the higher displacement values were reached for the lighter loads. The curves for increasing and decreasing loads did not match in either one of the tests and therefore hysteresis was exhibited. This was mainly attributed to the friction between the actuator and the casing around it [8]. In addition, the estimated pressure threshold values for each one of these actuators were estimated for the three different load conditions. These values corresponded to the minimum pressure input at which actuation begins. In order to calculate this minimum pressure, the inlet pressure was increased until actuation started to occur. Once a certain actuation was observed, the corresponding pressure readings were recorded. The results are presented in Table 3.

Table 3. Pressure threshold values for different load conditions.

Load (g)	*Pressure Threshold (psi)*
10	0.47
200	0.75
500	1

Step Response Test

These tests were performed by applying a step change in input pressure. These input pressures corresponded to 1.2 and 1.6 psi values. The position vs time graphs (Figure 12 and Figure 13) show the change in position before a steady state position value was reached for the actuation extension. These tests were carried out for the same three different loading conditions discussed in the previous section.

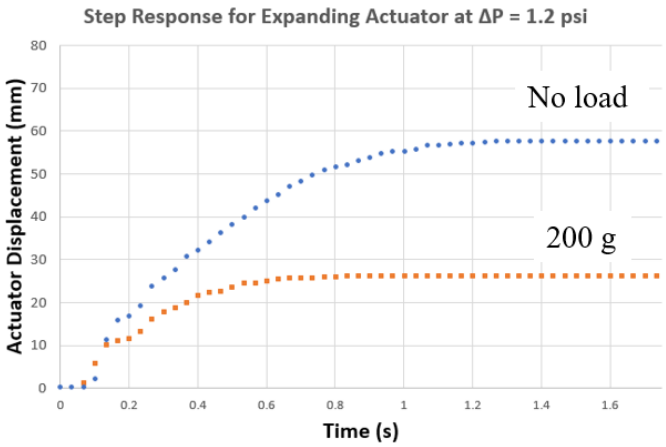

Figure 12. Step response for 1.2 psi input.

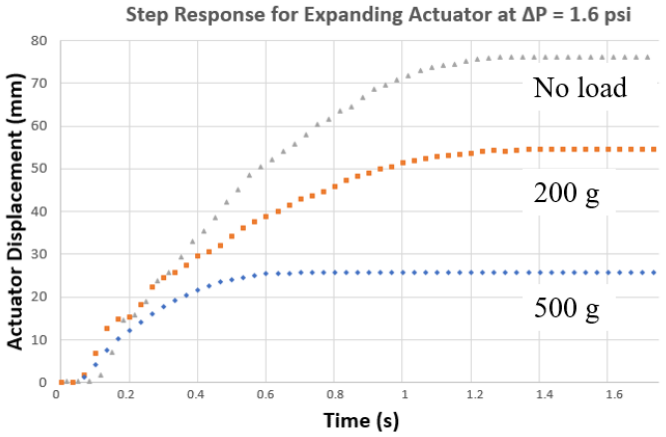

Figure 13. Step response for 1.6 psi input.

For the 1.6 psi pressure input as seen in Fig. 13, it was possible to obtain a specific actuator displacement for each of the different loads. However, for the 1.2 psi (Fig. 12) it was not possible to obtain any stable actuator displacement when loading the actuator with a 500g mass. Even though it was possible to move the weight a certain distance after overcoming the 1 psi pressure threshold, it was not possible to keep the load at this distance and the actuator came back to its original position after 10 seconds. This was mainly due to minor leakage in the several fittings and connections in the pneumatic setup. The settling times were also calculated. These were defined as the time it took for the actuation to expand from the initial position to be within a 2% error of the final, steady-state, position [9]. The results for these settling times are displayed in Table 4.

Copyright © 2018 ASME

Downloaded From: https://proceedings.asmedigitalcollection.asme.org on 11/20/2018 Terms of Use: http://www.asme.org/about-asme/terms-of-use

Table 4. Response time in dynamic response.

Pressure Input (psi)	Load (g)	Response Time (s)
1.2	No load	1.07
	200	0.70
1.6	No load	1.18
	200	1.13
	500	0.50

The results presented were used to confirm that it was possible to see that a higher pressure increased the settling time. In addition, a lower load increased the setting time as well. This was due to the fact that a higher pressure and lower load increased the position reached by the actuator. Due to this higher position, it took more time for the actuator to reach steady-state behavior.

CONCLUSIONS

This work has explored two methods to fabricate soft pneumatic actuators using 3D printing. The first one involved using a combination of resins to 3D print actuators directly using stereolithography. However, this printing methodology did not provide the possibility of fabricating actuators with the required durability and stroke. The second method involved making a mold using FDM and casting Ecoflex® 00-30 silicone. The first attempt involved making a 2-step mold, which caused detachment issues during testing. In the second attempt, this 2-step mold process was replaced by a single step process by using a soluble core. This provided a successful actuator. The steady state and dynamic response of this actuator were evaluated. Steady state results showed the presence of hysteresis, and demonstrated that a higher load resulted in a lower actuator displacement for the same pressure level. The pressure threshold levels were documented for each of the loading conditions. Regarding the dynamic response, two different pressure levels were evaluated. These results indicated that a lower load and a higher pressure resulted in a longer settling time to achieve maximum position.

ACKNOWLEDGEMENTS

This work has been supported by Otto Maha Endowement Grant. The authors would like to thank Laura D. Vallejo Mandalejo and Angello A. Vindrola Munoz for their assistance with the electronic equipment setup. Special thanks to Ross Grinvalds from ProportionAir for his support in the construction of the experimental setup.

REFERENCES

1. Heney, P. (2016, November 5). *What are pneumatic cylinders?* Retrieved from https://www.pneumatictips.com/what-are-pneumatic-cylinders/
2. Slightman, J. E., & Gervasi, V. R. (2012). Novel Integrated Fluid-Power Actuators for Functional End-Use Components and Systems via Selective Laser Sintering Nylon 12. *23rd Annual International Solid Freeform Fabrication Symposium - An Additive Manufacturing Conference.*
3. MacCurdy, R., Katzschmann, R., Kim, Y., & Rus, D. (2016). Printable Hydraulics: A Method for Fabricating Robots by 3D Co-Printing Solids and Liquids. *IEEE International Conference on Robotics and Automation.*
4. Peele, B. N., Wallin, T. J., Zhao, H., & Shepherd, R. F. (2020). 3D printing antagonistic systems of artificial muscle using projection stereolithography. *Bioinspir. Biomim. 10* .
5. Belforte, G., Eula, G., Ivanov, A., & Sirolli, S. (2014). Soft Pneumatic Actuators for Rehabilitation. *Actuators*.
6. Agarwal, G., Besuchet, N., Audergon, B., & Paik, J. (2016). Stretchable Materials for Robust Soft Actuators towards Assistive Wearable Devices. *Scientific Reports*.
7. Case, J. C., White, E. L., & Kramer, R. K. (2015). Soft Material Characterization for Robotic Applications. *SOFT ROBOTICS*, 80-87.
8. Chou, C. P., & Hannaford, B. (1996). Measuring and Modeling of McKibben Pneumatic Artificial Muscles. *IEEE Transactions on Robotics and Automation*, 90-102.
9. Christiansen, D., & Alexander, C. (2005). Control Systems. In *The Electronics Engineers' Handbook, 5th Edition* (pp. 19.1-19.30). McGraw-Hill.

Copyright © 2018 ASME

Downloaded From: https://proceedings.asmedigitalcollection.asme.org on 11/20/2018 Terms of Use: http://www.asme.org/about-asme/terms-of-use